PHYSICAL REVIEW B VOLUME 25, NUMBER 12 15 JUNE 1982

Thermodynamic properties of solid sodium from quasiharmonic lattice dynamics and molecular dynamics

Richard E. Swanson,* Galen K. Straub, Brad L. Holian, and Duane C. Wallace
Los Alamos National Laboratory, Los Alamos, New Mexico 87545
(Received 22 December 1981)

Quasiharmonic-lattice-dynamics and molecular-dynamics calculations were performed on metallic sodium from the low-temperature region to above melting at several different volumes. A pseudopotential model was used that consisted of a large volume-dependent potential plus a small effective two-body potential. From the molecular-dynamics results for the solid phase, we have constructed the Helmholtz free energy and calculated the thermodynamic properties up to the melting temperature. The anharmonic contributions to the internal energy and pressure are determined directly from molecular dynamics without using thermodynamic perturbation theory. Calculated and experimental values of the zero-pressure volume-temperature curve, isothermal bulk modulus, heat capacity, and Grüneisen parameter are found to be in good agreement. We conclude that the pseudopotential model provides an accurate representation of the potential for energies up to melt; molecular-dynamics simulations accurately represent the classical vibrational contributions to the thermodynamic functions at high temperatures and give a meaningful evaluation of the anharmonicity. The combination of quasiharmonic-lattice-dynamic theory in the quantum regime and molecular dynamics in the classical regime provide a simple and natural representation of the vibrational thermodynamics of a solid.

I. INTRODUCTION

In the theory of thermodynamic properties of solids there are two significant temperature ranges separated by the high-temperature harmonic Debye temperature $\Theta_{H\infty}$. For $T<\Theta_{H\infty}$, quantum effects are important, and thermodynamic functions depend strongly on the distribution of phonon frequencies. For $T\gtrsim\Theta_{H\infty}$, quantum effects are not important, but anharmonic contributions to thermodynamic functions have to be reckoned with. While anharmonicity is complicated in quantum theory and is generally treated as a perturbation, the technique of computer simulation treats the anharmonic motion of the atoms essentially exactly in classical statistics. It is therefore sensible to combine the two approaches, to use quasiharmonic lattice dynamics in the low-temperature range and classical computer simulation at high temperatures.

In the present work we are interested primarily in metals. Several computer simulations based on pseudopotential theory have been done. The Monte Carlo technique was used by Cohen and Klein[1] to study potassium at zero pressure, and by Cohen *et al.*[2] to study sodium at zero pressure. Rahman[3] examined density fluctuations in liquid rubidium by molecular dynamics, and MacDonald *et al.*[4] computed the anharmonic specific heat of solid rubidium by the Monte Carlo method. At Los Alamos, we have undertaken examination of the use of molecular dynamics to calculate thermodynamic properties of solid and liquid metals as functions of temperature and pressure. For this purpose we consider sodium, and we use a local pseudopotential theory for which extensive lattice-dynamics calculations were done previously. The present paper reports our results for bcc sodium at temperatures up to melting and at modest pressures.

II. METHOD

We have a system of N ions and zN electrons in a volume V. In the adiabatic approximation, the total energy is the sum of kinetic energies of all the ions, plus the total adiabatic potential Φ. If the zero of Φ corresponds to having neutral atoms infinitely separated, and I_z is the ionization energy, then in the pseudopotential perturbation formulation $\Phi-NI_z$ contains a volume-dependent term $\Omega(V)$ and a sum over all distinct pairs of ions of the effective ion-ion potential $\phi(r)$:

$$\Phi-NI_z=\Omega(V)+\sum\phi(r)\ . \tag{1}$$

Expressions for $\Omega(V)$ and $\phi(r)$ are[5]

$$\Omega(V)=zN\left[\tfrac{3}{5}\epsilon_F+\epsilon_X+\epsilon_C-\tfrac{1}{3}\epsilon_F+\frac{e^2f}{3\pi\zeta}\right]$$
$$+N\frac{V_A}{2\pi^2}\int_0^\infty F(q)q^2dq\ , \qquad (2)$$

$$\phi(r)=\frac{z^2e^2}{r}+\frac{V_A}{\pi}\int_0^\infty F(q)\frac{\sin qr}{qr}$$
$$\times q^2dq+\alpha e^{-\gamma r}\ . \qquad (3)$$

Here $\frac{3}{5}\epsilon_F+\epsilon_X+\epsilon_C$ is the kinetic plus exchange plus correlation energy per electron of a uniform electron gas, f is the free-electron Fermi wave vector, ζ is the parameter in the Hubbard form of the screening correction, $V_A=V/N$ is the volume per atom, and $F(q)$ is the energy-wave-number characteristic, which is quadratic in the pseudopotential. The band-structure energy has been transformed into the second term in (3), plus contributions to (2). The potential $\phi(r)$ depends on V, through the second term in (3), and it includes a Born-Mayer repulsion, the last term in (3). For the parameters in $\phi(r)$, we take those that were determined earlier by requiring agreement between theory and experiment for the crystal binding energy, and its first two volume derivatives, at zero temperature and pressure.[6] A graph of $\phi(r)$ for Na at $V_A=256a_0^3$ is shown in Fig. 1.

For the molecular-dynamics system, we take a cell containing 672 particles (ions) in a rectangular volume with periodic boundary conditions on all sides. Each particle is located on a bcc lattice site

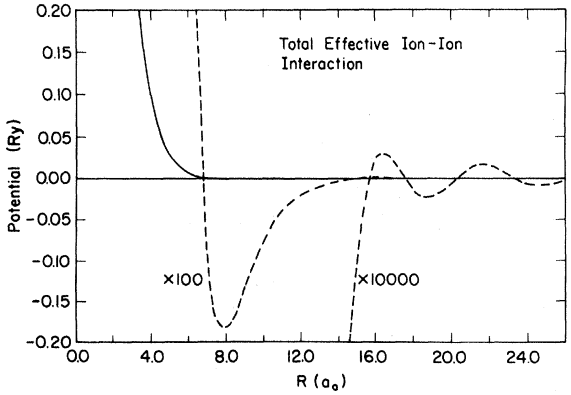

FIG. 1. Total effective ion-ion pair potential for Na calculated from a modified point-ion pseudopotential at a volume $V_A=256a_0^3$. The dotted lines are multiplied by the factor indicated near the curves. The potential energy is in units of rydbergs (Ry) and the separation is in units of Bohr radii (a_0).

at time $t=0$, and is given a random initial velocity. The coupled classical equations of motion are solved numerically for increasing time in the centered finite-difference approximation, with a time step approximately 1% of the mean vibrational period of the particles. Each calculation is performed under the constraints of constant volume and constant total energy. When the system is in equilibrium, the total energy is the thermodynamic internal energy U and the temperature T is related to the ensemble-average kinetic energy

$$kT=\tfrac{1}{3}M\langle v^2\rangle\ , \qquad (4)$$

where k is Boltzmann's constant, M is the particle mass, v is a particle velocity, and the brackets $\langle\ \rangle$ denote an ensemble average. Because $\phi(r)$ depends on V, the pressure P is given by

$$P=-\frac{d\Omega}{dV}+\frac{NkT}{V}-\left\langle\sum\left[\frac{\partial\phi}{\partial V}+\frac{r}{3V}\frac{\partial\phi}{\partial r}\right]\right\rangle\ . \qquad (5)$$

Again, the sum in (5) is over all distinct pairs of ions.

Because the initial distribution of particle velocities is not a Maxwell-Boltzmann distribution, the system is not initially in thermodynamic equilibrium. The approach to equilibrium can be observed in a graph of the "instantaneous temperature" $T(t)$, which is defined by (4) with $\langle v^2\rangle$ replaced by the system average of v^2 at time t. Figure 2 shows $T(t)$ for two different systems, with $T(0)$ only a few degrees apart. Upon equilibration, the higher-temperature system was in the fluid phase, while the lower-temperature system remained in the bcc crystalline phase. The figure shows a result characteristic of our calculations, namely that $T(t)$ increases toward equilibrium for the crystal, and decreases toward equilibrium for the fluid. The fourth-order cumulant of the velocity distribution is the kurtosis $C(t)$.[7] In equilibrium, the time average of $C(t)$ is zero for an infinite system, and slightly negative for a finite N. Figure 3 shows $C(t)$, scaled by T^2/N, for two systems in the solid phase; the function approaches zero rapidly in the first ten time steps, and then approaches its final value on approximately the same slow timescale as does $T(t)$.

We can gain insight into the molecular-dynamics results by comparing them with the classical limit (high-T limit) of lattice-dynamics theory. The high-T lattice-dynamics equation for the Helmholtz free energy F is a quasiharmonic term plus an anharmonic term F_A:

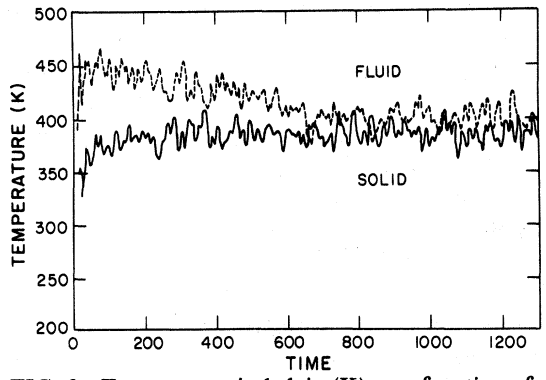

FIG. 2. Temperature in kelvin (K) as a function of time for the equilibration of two different molecular-dynamics calculations. The dashed curve is for a system that came to final equilibrium in the fluid phase while the solid curve remained in the solid phase.

$$F=\Phi_0-3NkT\ln(T/\Theta)+F_A\ , \tag{6}$$

where Φ_0 is $\Phi(T=0)$ and the classical characteristic temperature Θ is related to the phonon frequencies ω by

$$\ln k\Theta=\langle\ln\hbar\omega\rangle\ . \tag{7}$$

Here the brackets $\langle\ \rangle$ denote a Brillouin-zone average. Corresponding to F, the internal energy and pressure are

$$U=\Phi_0+3NkT+U_A\ , \tag{8}$$

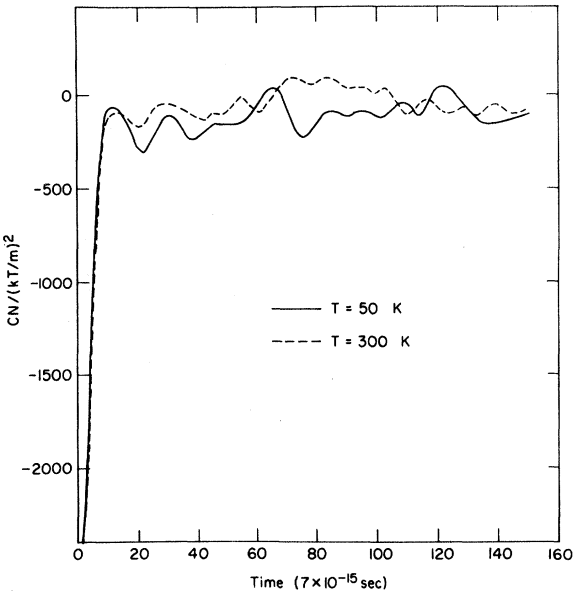

FIG. 3. Kurtosis C of the particle velocity distribution, scaled by T^2/N vs time during the equilibration of molecular-dynamics calculations at $T=50$ and 100 K. m is the particle mass.

$$P=-\frac{d\Phi_0}{dV}-3NkT\frac{d\ln\Theta}{dV}+P_A\ , \tag{9}$$

where

$$U_A=F_A-T\left[\frac{\partial F_A}{\partial T}\right]_V\ , \tag{10}$$

$$P_A=-\left[\frac{\partial F_A}{\partial V}\right]_T\ . \tag{11}$$

In these equations the anharmonic contributions are not necessarily small and are not necessarily expressed by perturbation theory. Thermodynamic contributions from electron excitation are negligible in the present calculations.

III. MOLECULAR-DYNAMICS RESULTS

Molecular-dynamics calculations were carried out for the three volumes $V_A=232$, 256, and 270 a_0^3. For each volume, the results for $U-NI_z$ as a function of T are shown by the points plotted in Fig. 4. At sufficiently high temperatures, the molecular-dynamics system automatically equili-

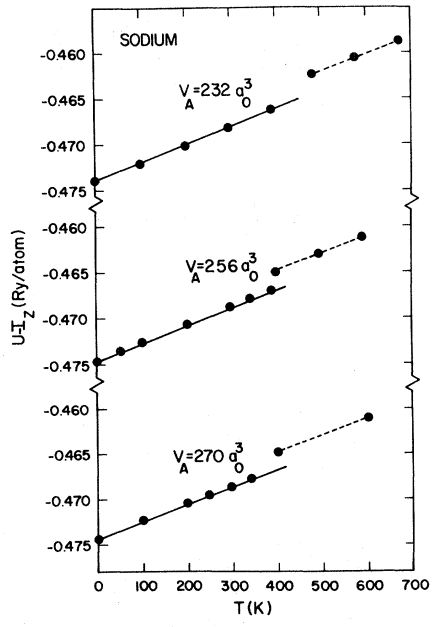

FIG. 4. Total internal energy per atom U minus the ionization energy I_z vs temperature from the molecular-dynamics calculations. The solid lines are the quasiharmonic part of Eq. (8) for U; i.e., they express the quantity Φ_0-NI_z+3NkT. The dashed lines through the fluid phase points are not theoretically derived curves.

TABLE I. Summary of the molecular-dynamics results for sodium.

T (K)	$V_A=232a_0^3$ $U-I_z$ (Ry/atom)	P (10^{-5} Ry/a_0^3)	T (K)	$V_A=256a_0^3$ $U-I_z$ (Ry/atom)	P (10^{-5} Ry/a_0^3)	T (K)	$V_A=270a_0^3$ $U-I_z$ (Ry/atom)	P (10^{-5} Ry/a_0^3)
0.0	−0.473 938	5.62	0.0	−0.474 539	−0.179	0.0	−0.474 341	−2.55
100.0	−0.472 032	6.53	50.1±0.1	−0.473 587	0.267±0.003	99.8	−0.472 444	−1.67
199.4	−0.470 112	7.44	100.1	−0.472 632	0.713	199.2±0.1	−0.470 532	−0.807±0.004
296.1±0.5	−0.468 220	8.33±0.01	199.4	−0.470 715	1.60	246.6	−0.469 593	−0.384
391.3	−0.466 311	9.32	295.1	−0.468 822	2.46	294.3	−0.468 640	0.005
478.2	−0.462 483	11.3	342.4±0.5	−0.467 861	2.90±0.01	340.3	−0.467 668	0.501
574.0	−0.460 585	12.1	385.1	−0.466 944	3.34	404.4	−0.464 812	2.03
672.4	−0.458 655	13.0	396.2	−0.464 999	4.46	502.2	−0.462 915	2.83
			493.2	−0.463 102	5.30	600.8	−0.461 018	3.64
			587.9±0.5	−0.461 215	6.12±0.02			

brated in the liquid phase; the corresponding points on each $U(T)$ graph are seen to lie on a line displaced upward from the solid-phase $U(T)$ curve. The solid lines in Fig. 4 are the quasiharmonic part of Eq. (8) for U, i.e., they express the quantity Φ_0-NI_z+3NkT. The dashed lines through the fluid points are not theoretically derived curves. The obvious conclusion from Fig. 4 is that the anharmonic contribution to the internal energy, U_A, is extremely small for bcc Na.

Again for each volume, the molecular-dynamics results for P as a function of T are shown by the points in Fig. 5, while the solid lines are the quasiharmonic terms from Eq. (9). As for the energy, the anharmonic contribution to the pressure is extremely small for bcc Na. Also for each volume the fluid points for $P(T)$ lie on a line displaced upward from the solid-phase $P(T)$ curve. All the molecular-dynamics data for solid and fluid Na are listed in Table I. We are continuing our study of the fluid phase, and will reserve further discussion of these results until later.

Even though the anharmonic contributions are small the molecular-dynamics calculations still contain accurate information about them. U_A and P_A are determined by subtracting the quasiharmonic contributions from the molecular dynamics results; the values obtained are shown in Figs. 6 and

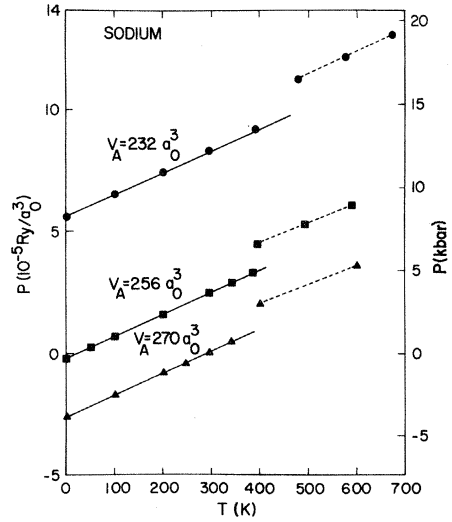

FIG. 5. Total pressure P vs temperature from the molecular-dynamics calculations. The solid lines are the quasiharmonic part of Eq. (9). The dashed lines through the fluid phase points are not theoretically derived curves. The scale on the right side is in units of kbar.

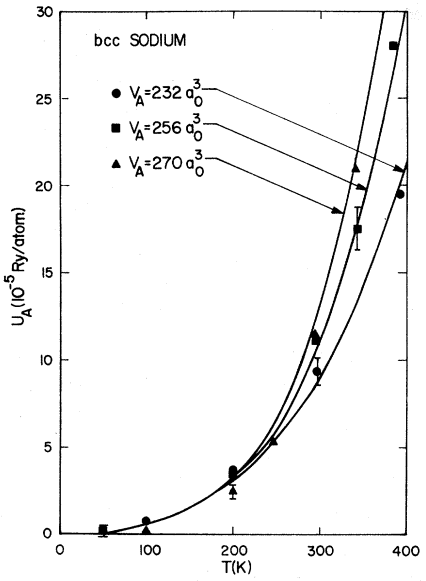

FIG. 6. Anharmonic contribution to the internal energy U_A vs temperature. The solid curves are from the fits to all the molecular dynamics results for the internal energy and pressure using the coefficients given in Eq. (12).

7. The error bars represent rms deviations from the mean, arising mostly from fluctuations in $T(t)$, and do not account for systematic errors. It is obvious that the constant-volume curves of U_A and P_A are not simply quadratic functions of T as is

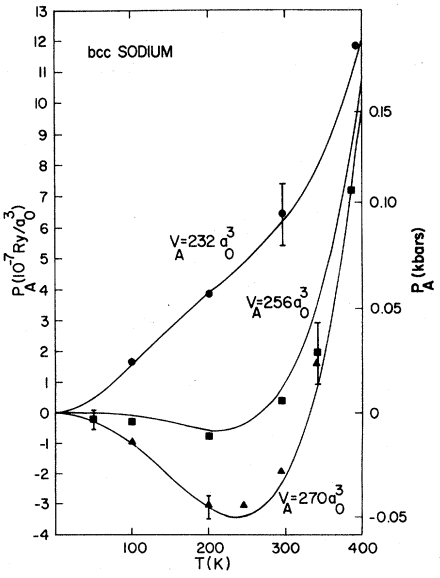

FIG. 7. Anharmonic contribution to the pressure P_A vs temperature. The solid curves are from the fits to all the molecular dynamics results for the internal energy and pressure using the coefficients in Eq. (12).

predicted by leading-order anharmonic perturbation theory. We were not able to discover a simple functional form for the anharmonic quantities, and so we attempted to fit the data by means of a power-series expression for F_A:

$$F_A = A_2 T^2 + A_3 T^3 + A_4 T^4 . \tag{12}$$

With each of the coefficients A_2, A_3, A_4 taken as a quadratic function of the volume, giving a total of nine fitting parameters, it is possible to obtain a good representation of all the anharmonic data, a total of 30 values of U_A and P_A at different volumes and temperatures. The fitted curves are shown by the lines in Figs. 6 and 7.

IV. COMPARISON WITH EXPERIMENT

In our computer simulations, every atomic cell in the crystalline phase is occupied; there are no vacancies. We therefore estimated the vacancy contribution to each thermodynamic function in the solid phase, and subtracted this from the experimental result, before comparing it with our calculations. Equations for the vacancy contributions are given by Schoknecht and Simmons.[8] For the vacancy formation energy ϵ and entropy σ we used the values $\epsilon = 0.354$ eV and $\sigma = 3.9k$, determined by the experiments of Feder and Charbnau[9] and of Adlhart *et al.*[10] As an estimate of the vacancy formation volume we used the measured self-diffusion volume,[11] which is $0.4V_A$. The vacancy corrections are quite small for Na at $P=0$, being essentially zero for T below 290 K, and at the melting point amounting to -0.03% for the volume, -0.5% for the isothermal bulk modulus B_T, -2.4% for the constant-pressure specific heat C_P, and -0.6% for the Grüneisen parameter γ. Another concern in comparing our calculations with experiment is that the stable phase of Na at low temperatures is hcp. In some cases, experimental values have been estimated for the bcc phase at low temperatures, and these are the values shown in the following figures.

The melting temperature of Na is $T_M = 371$ K, and the temperature which approximately separates quantum and classical regimes is $\Theta_{H\infty} = 167$ K.[5] Calculated and measured curves of the volume at $P=0$ are shown in Fig. 8; comparison of the two curves may be understood as follows. Neglecting anharmonicity, the lattice-dynamics expression for F at $T=0$ is $\Phi_0 + \frac{1}{2}\sum\hbar\omega$. At high temperatures the zero-point energy is explicitly cancelled, and

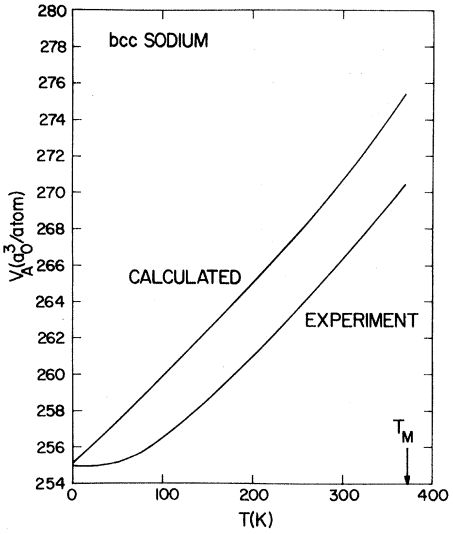

FIG. 8. Calculated and measured curves of the volume vs temperature at $P=0$.

the quasiharmonic F goes over to the classical expression $\Phi_0-3NKT\ln(T/\Theta)$. In the experimental curve of V vs T, Fig. 8, quantum effects are important at $T=0$ and at low T, in the region of strong curvature. Now when the model parameters for Na were determined some years ago,[6] the approximation was made of neglecting the zero-point energy compared to Φ_0. Hence the present classical calculation, in which $F=\Phi_0$ at $T=0$, agrees with the experimental volume at $T=0$; however, the present calculation does not reproduce the quantum low-T curvature in $V(T)$, but merely shows a roughly linear classical curve. We could construct a more accurate classical model by either including the zero-point energy in the fitting of model parameters at $T=0$, or by fitting the parameters to experiment in the classical region. In any case the discrepancy between calculation and experiment in Fig. 8 is not serious, the two volumes differing by $\lesssim 1.7\%$. We note that the anharmonic contribution to the calculated zero-pressure volume for Na is negligible. Also the fact that the two curves in Fig. 8 are nearly parallel means that our calculated thermal expansion coefficient is about the same as experiment for $T\gtrsim\Theta_{H\infty}$.

In Fig. 9, a collection of experimental values[12–16] of the isothermal bulk modulus is shown by the plotted points (adiabatic moduli were converted to isothermal where necessary). There is overall good agreement among the various experiments. The calculated classical curve of B_T at $P=0$ is shown by the solid line in Fig. 9; also, the

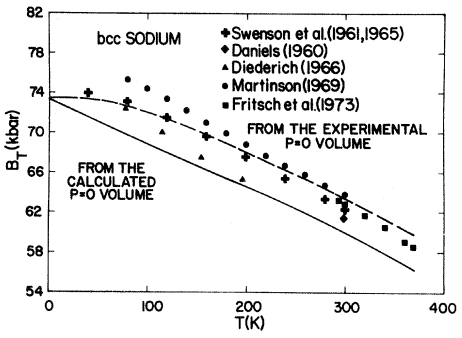

FIG. 9. Isothermal bulk modulus B_T vs temperature. The solid curve is from the calculated $P=0$ volume and the dashed curve is from the experimental $P=0$ volume as given in Fig. 8.

dashed line shows our evaluation of B_T at the *experimental* volume corresponding to $P=0$. The agreement between the calculations and the experiment is remarkably good. The anharmonic contribution to B_T is not entirely negligible, and amounts to about 1.2% for temperatures from around 200 K to T_M.

The heat capacity of solid sodium was measured by Filby and Martin[17] and Martin.[18,19] In Fig. 10 the measured C_P is shown, and also our estimated vacancy correction, as well as two theoretical curves. The curve labeled quantum theory is obtained from quasiharmonic lattice dynamics, and the classical curve shows our molecular-dynamics evaluation. The quantum and classical curves nearly intersect at 225 K.

Experimental data for the thermal expansion coefficient β of crystalline sodium exist for T

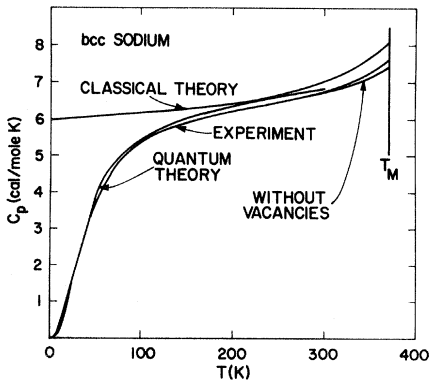

FIG. 10. Heat capacity at constant pressure C_p from classical theory using molecular dynamics and quantum theory using quasiharmonic lattice dynamics compared with experiment. The experimental results have been corrected to the case without vacancies as indicated near T_M.

above 80 K.[20–22] Corresponding to these data, values of the Grüneisen parameter $\gamma = V\beta B_T/C_V$ are shown by the points in Fig. 11. To calculate γ from molecular dynamics we used the equivalent expression $\gamma = V(\partial P/\partial U)_V$, and the result at $P=0$ is shown by the solid line in Fig. 11. The theory is in excellent agreement with the experiments, except possibly for T below 100 K. The anharmonic contribution to γ, which arises from both P_A and U_A in $(\partial P/\partial U)_V$, is small for $T \lesssim 200$ K, and then increases to 7% at T_M.

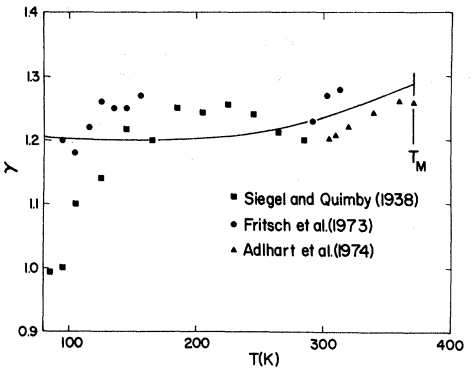

FIG. 11. Grüneisen parameter γ vs temperature. The points shown are determined from experimental values of the thermal expansion, isothermal bulk modulus, and heat capacity at constant volume.

V. CONCLUSIONS

We can make the following conclusions, based on the overall comparison of theory and experiment, and the internal consistency of the pressure and energy calculations.

(1) The pseudopotential model we are using provides an accurate representation of the large potential $\Omega(V)$ and the small effective two-body potential $\phi(r;V)$ for Na at $V_A = 232 - 270a_0^3$ and at energies up to kT_M.

(2) Given the potential $\phi(r;V)$, molecular-dynamics simulations accurately represent the classical vibrational contributions to thermodynamic functions, and give a meaningful evaluation of the anharmonicity even when this is very small (in the present work the anharmonic contributions to P and U are at most 3% and 4%, respectively, of the total vibrational contributions).

(3) The combination of quasiharmonic-lattice-dynamics theory in the quantum regime and molecular dynamics in the classical regime provide a simple and natural representation of the vibrational thermodynamics of a solid (as shown especially in Fig. 10 for the specific heat).

ACKNOWLEDGMENTS

We would like to thank J. D. Johnson for valuable comments and discussions. This work was supported by the U. S. Department of Energy and the U. S. Department of Air Force, Air Force Institute of Technology.

---

*Portions of this work are contained in a thesis for the University of New Mexico, Department of Physics and Astronomy. Present address: U. S. Air Force Academy, Colorado 80840.

[1]S. S. Cohen and M. L. Klein, Phys. Rev. B 12, 2984 (1975).
[2]S. S. Cohen, M. L. Klein, M. S. Duesbery, and R. Taylor, J. Phys. F 6, 337 (1976).
[3]A. Rahman, Phys. Rev. A 9, 1667 (1974).
[4]R. A. MacDonald, R. D. Mountain, and R. C. Shukla, Phys. Rev. B 20, 4012 (1979).
[5]D. C. Wallace, *Thermodynamics of Crystals* (Wiley, New York, 1972).
[6]D. C. Wallace, Phys. Rev. 176, 832 (1968).
[7]G. K. Straub, B. L. Holian, and R. G. Petschek, Phys. Rev. B 19, 4049 (1979).
[8]W. E. Schoknecht and R. O. Simmons, in *Thermal Expansion—1971*, edited by M. G. Graham and H. E. Hagy (AIP, New York, 1972), p. 169.
[9]R. Feder and H. P. Charbnau, Phys. Rev. 149, 464 (1966).
[10]W. Adlhart, G. Fritsch, and E. Lüscher, J. Phys. Chem. Solids 36, 1405 (1975).
[11]R. A. Hultsch and R. G. Barnes, Phys. Rev. 125, 1832 (1962).
[12]R. I. Beecroft and C. A. Swenson, J. Phys. Chem. Solids 18, 329 (1961).
[13]W. B. Daniels, Phys. Rev. 119, 1246 (1960).
[14]M. E. Diederich and J. Trivisonno, J. Phys. Chem. Solids 27, 637 (1966).
[15]R. H. Martinson, Phys. Rev. 178, 902 (1969).
[16]G. Fritsch, F. Geipel, and A. Prasetyo, J. Phys. Chem. Solids 34, 1961 (1973).
[17]J. D. Filby and D. L. Martin, Proc. R. Soc. London, Ser. A 276, 187 (1963).
[18]D. L. Martin, Proc. R. Soc. London, Ser. A 254, 433

(1960).
[19]D. L. Martin, Phys. Rev. 154, 571 (1967).
[20]S. Siegel and S. L. Quimby, Phys. Rev. 54, 76 (1938).
[21]G. Fritsch, M. Nehmann, P. Korpiun, and E. Lüscher, Phys. Status Solidi A 19, 555 (1973).
[22]W. Adlhart, G. Fritsch, A. Heidemann, and E. Lüscher, Phys. Lett. 47A, 91 (1974).